

A Knee-based Multi-objective Optimization for Gait Cycle of 25-DOF NAO Humanoid Robot

Pushpendra Gupta¹, Dilip Kumar Pratihar¹, and Kalyanmoy Deb²

¹ Mechanical Engineering Department, Indian Institute of Technology Kharagpur,
West Bengal 721302, India

pushpendra050@iitkgp.ac.in, dkpra@mech.iitkgp.ac.in,

² Electrical and Computer Engineering, Michigan State University,
East Lansing, MI 48824, USA
kdeb@egr.msu.edu

COIN Report 2025008

Abstract. A multi-objective optimization problem finds multiple optimal solutions represented on a Pareto front (PF), for conflicting objectives. Focusing on the "knee" region (KR) of the PF is preferred to targeting the entire PF since there is a significant degradation in one objective for a minor gain in another outside the KR. This paper applies two knee-finding methodologies— angle- and utility-based methods within the elitist non-dominated sorting genetic algorithm (NSGA-II), to address a multi-objective optimization problem of a 25 DOF NAO humanoid robot's gait cycle. The objectives are minimizing power consumption and maximizing dynamic balance margin. The single support phase exhibits a single KR, whereas the double support phase shows two KR. This research demonstrates a knee-based multi-objective optimization algorithm to reduce the burden on decision-makers in selecting the most preferred solutions. It compares two knee-finding techniques and provides insights into a practical robotics problem for different gait cycle phases.

Keywords: NAO humanoid robot, multi-objective optimization, decision making, NSGA-II, knee-based evolutionary algorithm.

1 Introduction

Evolutionary Multi-objective optimization (EMO) techniques are often used to simultaneously optimize several objectives that may be in conflict with each other. EMO finds multiple solutions, known as "Pareto optimum solutions," representing a trade-off between conflicting objectives. While the Pareto optimum solutions are not inferior to one another, it can be challenging for the decision maker (DM) to select the best solution out of many options. However, if the Pareto Front (PF) has a "knee" region (KR), they often draw the attention of DMs, as it helps narrow down the options. A knee region is one outside that a slight enhancement in one objective is accompanied by a substantial worsening

in another objective. In such cases, it is better to search this region of interest instead of the whole PF. However, some prior information about the existence of a knee region is not usually available to the DM. Researchers employed various multi-criterion decision-making techniques to focus on a preferred region of the PF. Angle and utility-based knee-finding methods [4] enable the DM to make the better choices from the fewer solutions without having prior knowledge of the importance of different objectives, which is not possible in real-world problems. Thus, angle- and utility-based methods are utilized to directly find the KRs instead of the whole PF.

Researchers have made significant progress in finding the PF solutions using EMO techniques. The majority of the effort in multi-objective optimization using EMO approaches had been concentrated on determining the optimal PF. This advancement has resulted in several efficient metaheuristic and population-based algorithms for dealing with competing objectives. Open-source programs such as jMetal [11], jMetalpy [2], PyGMO [23], Platypus [15], pymoo [3] and Metaheuristics [16], and commercial software like Matlab, Wolfram Mathematica etc., could handle the optimization requirements. However, presenting the trade-off solution set was not sufficient; much work is still necessary to integrate the decision-making processes. Designers must explore the design space to make the better-informed selections, and selecting a preferred solution set would benefit DM. The Knee solutions help concentrate on one or more regions of interest. The procedure can be repeated as often as necessary until DM is satisfied with the final outcome. Decision-making and optimization are dependent activities that cannot be considered separately. The DM can choose between solutions before, during, or after optimization. During the optimization process, these choice categories are referred to as a priori, progressive, and posteriori [33]. Most EMO approaches are posteriori, meaning that the DM makes his/her decision after receiving trade-off solutions. These decisions get considerably more challenging when dealing with multi-objective optimizations. This paper attempts to reduce the burden of DM by providing the fewer solutions.

Problems related to biped locomotion are increasingly solved for competing objectives like power and stability using EMO [9, 20, 21, 25, 26]. A gait cycle that is energy efficient and ensures a significant level of stability, leading to a smooth walking motion, is considered to be the most desirable. The DM favors design parameters that can accomplish the task with higher stability and lower energy usage. This research attempts to determine optimum gait parameters that decrease power utilization while enhancing the stability of the NAO. The multi-objective optimization problem is addressed using the elitist non-dominated sorting genetic algorithm-II (NSGA-II) [8] to find PF separately during the single support phase (SSP) and double support phase (DSP). This problem formulation also considers maintaining torque variation within a predefined threshold. In this paper, an endeavor has been put forward to incorporate the knee-based methods in this problem for finding knee solutions, which will assist the DM in selecting a preferred one from a few alternate solutions compared to the entire PF. Two knee-finding methodologies have been implemented separately in NSGA-

II to solve the optimization problem during each phase. SSP exhibits a single knee-like region, whereas DSP shows two. First, it is tested on a benchmark test problem and later implemented on the NAO robot gait generation problems. Overall, besides comparing two knee-finding methods, this study demonstrates the application of a knee-based EMO algorithm to focus on the interested region, revealing interesting insights into the robotics problem.

The rest of the paper is organized as follows: Section 2 presents key past studies on knee-finding methods. Section 3 discusses the knee-finding methodologies used in this paper. Then, Section 4 introduces the gait generation problem. Section 5 presents the mathematical multi-objective optimization problem formulation. Results are presented in Section 6. Finally, conclusions are made in Section 7.

2 Past Studies

Das [5] first identified the knee as a desired or good PF region. Branke et al. [4] modified the EMO method to focus on knee regions utilizing angle and utility-based focus. This assisted in narrowing the search region and generating fewer but more relevant DM solutions. DO-DK and DEB-DK were also proposed in [4] as benchmark problems and performance metrics to test the knee-based EMO algorithms. Another research used trade-off information to describe the knee [24]. Test problems with complicated knee regions were created to evaluate EMO algorithms' capacity to detect all knee points [37]. Deb and Gupta [7] offered multiple definitions for knee points and knee regions, as well as edge knee solutions for bi-objective problems and properties of such problems that may exhibit a Knee solution. Afsar et al. [1] presented an artificial decision maker (ADM) to quantitatively evaluate several reference point-based EMO approaches. The ADM process involves generating reference points in a learning phase to gain insight into the problem and in a decisive phase to designate a region of interest. It was found to be effective in comparing different EMO algorithms. Zhang et al. [38] proposed an EMO (MMO-EvoKnee) to search for the whole set of global knee solutions rather than an entire PF. Their study of various problems demonstrates that the proposed method can lessen the burden of the DM. He also proposed a recursive evolutionary algorithm (EvoKnee^r) [39] for finding both local and global knee solutions.

The impact of a knee-based algorithm is demonstrated by solving a complex gait cycle problem for the NAO humanoid robot. SSP and DSP represent the phases when the NAO is supported by a single leg and both legs, respectively [22]. Researchers had extensively focused on the influence of SSP [31, 35, 36], DSP [26], and both phases [19] for highly stable and efficient gait cycle. However, DSP occurs for a short period of time and has received less attention compared to SSP. DSP was simplified by modeling it as an Inverted Pendulum in [19], whereas Rajendra and Pratihari [26] investigated it as two SSPs with no lateral movement. Raj et al. [25] demonstrated a trade-off between stability and energy consumption in optimizing walk parameters for the NAO robot. Still, their study

assumed a constant hip height of the NAO robot. Genetic algorithms (GA) [6,9,13] extensively had been used by researchers to find the best trajectories for efficient gait cycles. Few notable research to reduce the high energy consumption could be found in [18,28,32], and Uno et al. [32] also considered the least change in torque for smoother motion.

This research aims to address gaps in the field of biped robot gait optimization by examining the DSP, lateral movement, and the effect of arm and hip movements in 3-dimensional space on stability. Moreover, most knee-finding methods are tested on benchmark problems, but an application to a complex real-world problem may provide more insight into the effectiveness of these methodologies. The effectiveness of knee-finding techniques, viz. angle, and utility-based methodologies is evaluated through testing on benchmark problems and application to a complex real-world problem involving the bipedal gait cycle. It allows for exploring the relevant knee region to understand the optimization problem in robotics better. Thus this paper focuses on the relevant knee region using angle and utility-based methodologies to provide valuable insights into the robotics optimization problem.

3 Knee Based Optimization Methodology

EMO generates a set of solutions known as Pareto optimal solutions, but these solutions can be numerous and overwhelming for the DM. To reduce the burden on the DM, it can be useful to explore "knee" solutions, which are a small number of solutions near the true PF that offer a good trade-off between the objectives. However, it is not always possible for the DM to have access to the necessary information to identify good solutions in real-world problems, where the true PF is unknown. In these cases, angle- and utility-based methods [4] can be used to find knee solutions without requiring prior knowledge. NSGA-II [8] is a well-known EMO approach recognized for its rapid convergence towards PF while keeping a wide range of solutions. The two measurements, non-domination rank, and crowding distance, assist in achieving those quality features. The second measurement in the algorithm is modified to focus on the knee and replaced with angle and utility-based techniques.

3.1 Angle-Based Focus

This allows the EMO approach to focus on the knee area without needing prior knowledge. The slope of the lines connecting an individual solution with its two neighbors can be used to estimate the degree of trade-off in either direction. The angle formed by these slopes can then be used to determine if the solution is at the knee, which is considered a desirable region for decision-making.

The angle α for a PF with a knee is shown in Fig. 1(a). It is a slope obtained by taking into consideration just one neighboring point. On the other hand, more intense bulges may be easily detected by taking more than two neighbors at a time, and the angles β , γ , and δ are computed by taking out two, three, and

four neighbors at a time, respectively. The larger angle indicates the larger bulge in the PF. Later, a benchmark test problem DO2DK with 1000 solutions in PF was explored. All slope angles are calculated directly using these solutions on the PF and shown in Fig. 1(b). Knee solutions can be obtained by including all slope angles slightly greater than 180° . However, four-angle measurement (when taken maximum of 4 angle measure) is more effective at identifying knee solutions than single-angle measurements due to the greater slope angle at the knee point. Figs. 1(c) and (d) depict the acquired knee solutions when all angles slightly greater than 180° are included during single-angle and four-angle measurements, respectively. The size of the markers grows in proportion to the slope angles. The largest value of these four angles is examined in Fig. 1(d), which focuses aggressively on knee solutions.

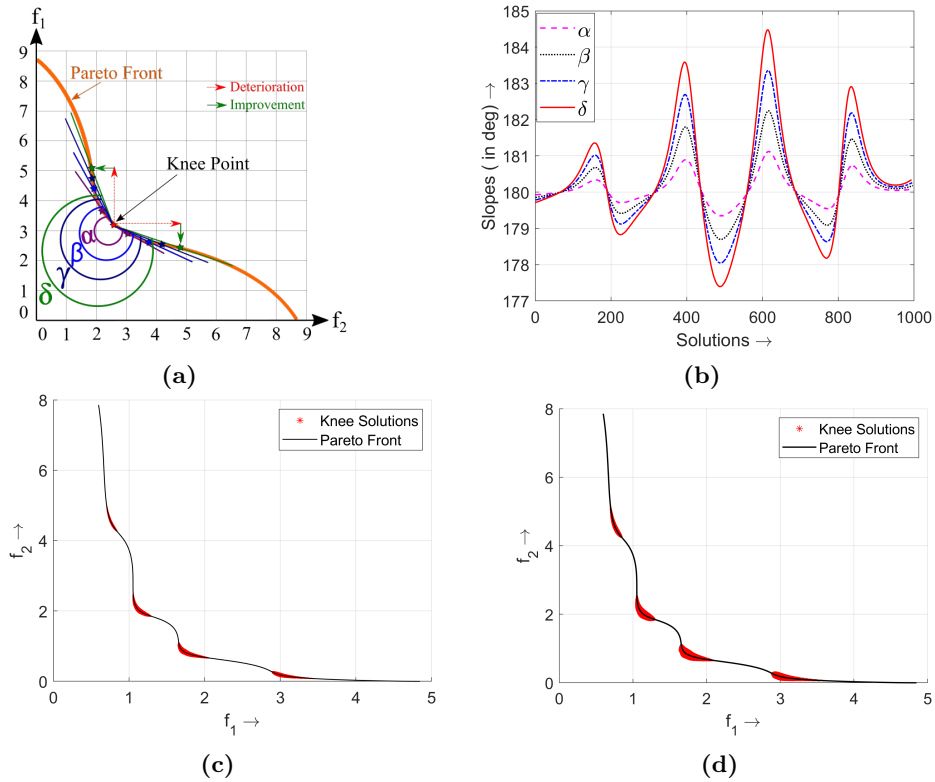


Fig. 1: Angle-based focus. **a** calculation of the angles viz. α , β , γ , and δ by taking 1, 2, 3 and 4 neighbours, respectively [4]. **b** variation of α , β , γ , and δ for DO2DK test problem. **c** knee solutions with single angle measure ($\alpha > 180.1^\circ$). **d** knee solutions with a maximum of 4 angle measures. ($\max(\alpha, \beta, \gamma, \delta) > 180.3^\circ$).

3.2 Utility-Based Focus

The expected marginal utility can be another way to find knee solutions. Suppose $U(x, \lambda) = \lambda f_1(x) + (1 - \lambda)f_2(x)$ is a known utility function $\forall \lambda \in [0, 1]$, then the DM can easily make his decision based on the highest utility. x_i denotes the solution at position i in the population for the objective f_1 .

$$\lambda_{i,j} = \frac{f_2(x_j) - f_2(x_i)}{f_1(x_i) - f_1(x_j) + f_2(x_j) - f_2(x_i)} \quad (1)$$

$$E(U'(x_i, \lambda)) = \int_{\lambda_{i-1,i}}^{\lambda_{i,i+1}} \alpha (f_1(x_i) - f_1(x_{i-1})) + (1 - \alpha) (f_2(x_i) - f_2(x_{i-1})) d\alpha \quad (2)$$

If it is sorted according to criterion f_1 , then $\lambda_{i,j}$ be the weighting of the ob-

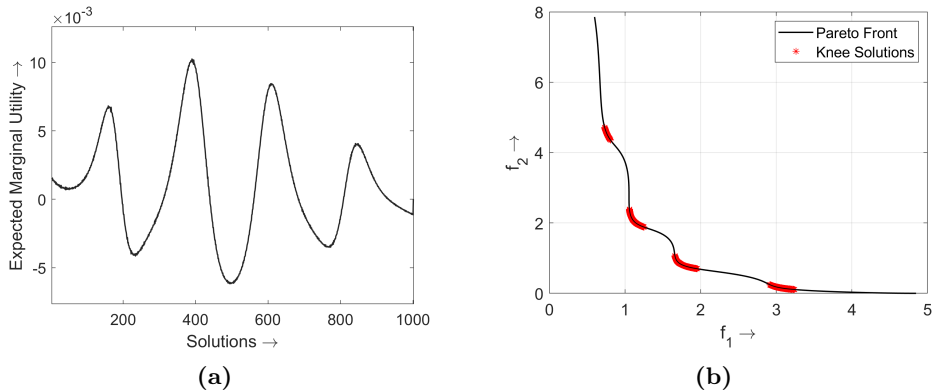


Fig. 2: Utility-based focus. **a** expected marginal utility variation. **b** mapping of utility function on the test problem to find the knee solutions.

jectives such that solutions x_i and x_j would have the same utility as given in (1). Then the expected marginal utility of the solution x_i can be calculated as given in (2) by integrating over all possible linear utility functions. $U'(x_i, \lambda)$ is the individual's marginal utility. This individual's marginal utility, as defined in an earlier publication [4], can act as an additional cost that the DM must bear in the absence of a particular solution. This approach may readily be expanded to more than two objectives by defining $U(x, \lambda) = \sum \lambda_i f_i(x)$ with $\sum \lambda_i = 1$. Multiple utility functions are first examined, and then an expected marginal utility is determined for the benchmark problem DO2DK with four knee solutions, as illustrated in Fig. 2(a). Later, a threshold value (equal to the mean of the utility functions) is used in the test problem to find four knee solutions, as shown in Fig. 2(b). In contrast to the angle-based method, the predicted utility function fluctuates with neighboring points since it is the additional cost the

DM must incur if that specific individual is unavailable, and the DM must settle for the second-best solution with the lower utility value. The utility-based NSGA-II knee solutions have been found to be more uniformly distributed than the angle-based technique, which intensifies at larger slope angles.

4 Problem Definition

In this section, the multi-objective optimization problems of gait generation have been introduced for the robot. The kinematic model and key parameters of NAO's walking gait are as described in detail in our prior work on single objective optimization [14]. In particular, the single and double support phases that characterize NAO's gait cycle were established in that paper. Building upon that foundation, here the approach has been extended to handle multiple competing objectives related to power consumption and dynamic stability.

All masses exerting force on the NAO robot's joint are taken into consideration [30]. Fig. 3(a) illustrates the NAO robot during SSP. Robot kinematics analysis is carried out using Denavit–Hartenberg parameters [10]. Inverse kinematics (IK) [14] determines the joint angles from the predefined cubic polynomial trajectories for the hip and swing leg. If $[X_{\text{Swing}}(t), -0.05, Z_{\text{Swing}}(X_{\text{Swing}})]^T$ and $[X_{\text{Hip}}(t), Y_{\text{Hip}}(t), Z_{\text{Hip}}(t)]^T$ denote the Swing leg ankle and hip Trajectories, respectively, then, four boundary conditions, $X_{\text{Swing}}(t_i) = x_i$, $X_{\text{Swing}}(t_f) = x_f$, $\dot{X}_{\text{Swing}}(t_i) = 0$, $\dot{X}_{\text{Swing}}(t_f) = 0$ are used to find the x -coordinates of the swing leg ankle. Its z -coordinates are found using $Z_{\text{Swing}}(x_i) = 0$, $Z_{\text{Swing}}(x_i + S_L) = 0$, $Z_{\text{Swing}}(x_m) = S_h^{max}$, $\dot{Z}_{\text{Swing}}(x_m) = 0$. t_i and t_f are the initial and final times during one gait cycle. Step length (S_L) is set to 0.06 m . Similarly, $X_{\text{Hip}}(t)$ (using $X_{\text{Hip}}(t_i) = x_i + x_f/4$, $X_{\text{Hip}}(t_f) = x_i + 3x_f/4$, $\dot{X}_{\text{Hip}}(t_i) = V_x^{\text{start}}$, $\dot{X}_{\text{Hip}}(t_f) = V_x^{\text{end}}$), $Y_{\text{Hip}}(t)$ (using $Y_{\text{Hip}}(t_i) = 0.025 m$, $Y_{\text{Hip}}(t_f) = 0.025 m$, $\dot{Y}_{\text{Hip}}(t_i) = V_y^{\text{start}}$, $\dot{Y}_{\text{Hip}}(t_f) = V_y^{\text{end}}$), and $Z_{\text{Hip}}(t)$ (using $Z_{\text{Hip}}(t_i) = h$, $Z_{\text{Hip}}(t_f) = h$, $\dot{Z}_{\text{Hip}}(t_i) = V_z^{\text{start}}$, $\dot{Z}_{\text{Hip}}(t_f) = V_z^{\text{end}}$) are calculated using their respective boundary conditions. h represents the hip height. The support leg is fixed at $[x_i + x_f/2, 0.05, 0]^T$. V_x^{start} , V_y^{start} and V_z^{start} are the starting velocities in x , y , and z -directions, respectively. V_x^{end} , V_y^{end} and V_z^{end} are the end velocities in x , y , and z -directions, respectively. The hip traveled from $X_{\text{Hip}}(t_i)$ to $X_{\text{Hip}}(t_f)$. Shoulder Pitch ($\theta_{SP}(t)$) and Elbow Roll ($\theta_{ER}(t)$) cubic trajectories are also considered in joint space during SSP. Both arms start with zero initial velocity and end at zero final velocity. Other four boundary conditions, $\theta_{\text{ShoulderPitch}}(t_i) = q_i^{SP} \text{ rad}$, $\theta_{\text{ShoulderPitch}}(t_f) = q_f^{SP} \text{ rad}$, $\theta_{\text{ElbowRoll}}(t_i) = q_i^{ER} \text{ rad}$, $\theta_{\text{ElbowRoll}}(t_f) = q_f^{ER} \text{ rad}$ are utilized to compute arm joint angles at a given time. The Lagrange-Euler formulation [12] is used to compute torque as $\tau_i = \sum_{c=1}^n D_{ic}\ddot{q}_c + \sum_{c=1}^n \sum_{d=1}^n h_{icd}\dot{q}_c\dot{q}_d + C_i$. D_{ic} , h_{icd} and C_i represent inertia, coriolis and centrifugal, and gravity terms, respectively. \dot{q}_i and \ddot{q}_i are the angular velocity and acceleration of the i^{th} joints.

The zero moment point (ZMP) [34] is the location on the ground where the total moments acting on the robot's body are balanced. At the ZMP, the robot

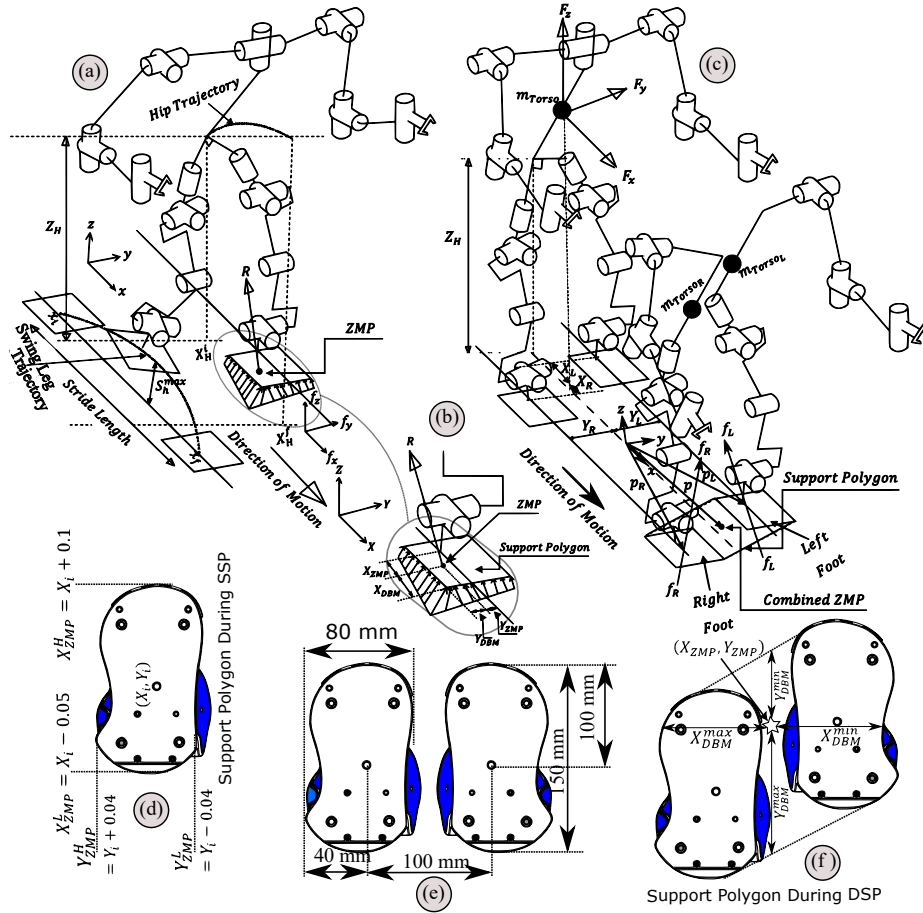


Fig. 3: Showing various aspects of bipedal locomotion of humanoid robot. **a** a schematic view during SSP. The stride length is from x_i to x_f whereas Z_H and S_h^{max} represent the hip height and maximum swing height, respectively. **b** definition of ZMP and DBM. **c** a schematic view during DSP. **d** ZMP's maximum and minimum values depend on the support leg location. **e** NAO robot foot dimensions. **f** minimum X_{DBM} and Y_{DBM} values during DSP.

is in dynamic equilibrium and will not fall over. The net moment occurs at the ZMP and is represented by the resultant force R , which must remain inside the foot support polygon to maintain the dynamic balance of the humanoid robot, as depicted in Figs. 3(a) and (b). ZMP along the x and y -axes can be determined [22] as $X_{ZMP} = \sum_{i=1}^{i=n} (I_i \dot{\omega}_i + m_i x_i (\ddot{z}_i - g) - m_i \dot{x}_i z_i) / \sum_{i=1}^n m_i (\ddot{z}_i - g)$ and $Y_{ZMP} = \sum_{i=1}^{i=n} (I_i \dot{\omega}_i + m_i y_i (\ddot{z}_i - g) - m_i \dot{y}_i z_i) / \sum_{i=1}^n m_i (\ddot{z}_i - g)$. All symbols carry their usual meaning. Figs. 3(d) and (e) show the lower and upper bounds of ZMP values based on the foot coordinates and the foot dimensions. The DBM [27] can be determined by calculating the absolute value of the difference between the ZMP and the edge of the support polygon. The DBM in the x direction (X_{DBM}) and y direction (Y_{DBM}) depend on the position of the support leg and the ZMP locations in each direction [14]. Initially, the combined center of mass of the entire robot is calculated, and its differentiation yields the total momentum of the robot. The equation of translational motion is determined by taking the numerical differentiation of total momentum with respect to time. This equation is then utilized to determine the external force experienced by the robot. Moreover, Gupta et al. [14] explored this approach on the NAO robot, and further detailed analysis is available in their work.

Fig. 3(c) shows the NAO robot model during DSP. The DSP is assumed as two SSPs using the Gupta et al. concepts [14]. The robot model consists of 23 lumped masses and is represented as two 12-mass serial manipulators. m_{Torso} , acting on both legs during DSP, is distributed in two parts, namely $m_{TorsoR} = m_{Torso} Y_R / (Y_L + Y_R)$ and $m_{TorsoL} = m_{Torso} Y_L / (Y_L + Y_R)$. $[X_L, X_R]^T$ and $[Y_L, Y_R]^T$ represent the distance of m_{Torso} on the ground from the left and right foot in the sagittal and lateral plane, respectively. The subscripts L and R have been used to denote the left and right leg, respectively. Two ZMP positions: p_L and p_R are initially determined after considering them as two SSPs, as shown in Fig. 3(c). The value of n is taken as 12 during ZMP calculations. m_{Torso} is replaced by either m_{TorsoL} or m_{TorsoR} , depending on which leg is being analyzed while computing the ZMP.

The whole model's ZMP at point p during DSP is calculated by putting the moment's x and y components about point $p = [p_x, p_y, 0]^T$ to zero [17]. The point p_L and p_R are the ZMP points for the respective legs and are obtained after solving for $p_x = (p_{Lx} f_{Lz} + p_{Rx} f_{Rz}) / (f_{Lz} + f_{Rz})$ and $p_y = (p_{Ly} f_{Lz} + p_{Ry} f_{Rz}) / (f_{Lz} + f_{Rz})$ [14]. DBM during DSP is determined, as shown in Fig. 3(f). The DBM is determined during hip movement from $[0.07, 0.025, h]^T$ to $[0.11, -0.025, h]^T$ during DSP by considering the minimum DBM available in the sagittal and lateral direction. Cubic polynomial functions are used to model the joint space trajectories for the shoulder pitch and elbow roll. The unknown coefficients in these cubic polynomials are determined by applying boundary conditions related to the start and end positions, as well as the start and end velocities that have been set to zero.

5 Multi Objective Optimization Formulation

In this paper, the gait cycle of the NAO robot is formulated as a multi-objective optimization problem to handle conflicting objectives viz. power consumption and stability margin with constraints in a 3D space with arms movement during each phase separately. The constraints include joint rotation limit, minimum torque fluctuation, minimum dynamic stability, a directional limit on hand movement, and minimum dynamic stability margin in the lateral direction.

The left leg (Support leg) during SSP is fixed at $[0.06, 0.05, 0]^T$. The Right leg (swing leg) moves from $[0.0, -0.05, 0]^T$ to $[0.12, -0.05, 0]^T$. In the context of gait analysis, the calculation of power consumption serves as the primary objective function. This involves determining the average power for j^{th} joint over an entire gait cycle duration, denoted as T . The power at each time step is computed by multiplying the joint torque (τ_j) and velocity (\dot{q}_j), and also accounting for heat loss, with a constant value of K set to 0.025. The objective is to minimize this function, denoted as P . Additionally, the optimization problem involves a secondary objective function that aims to maximize the stability margin. This multi-objective problem formulation specifically pertains to the single support phase and is represented by (3) and (4).

$$\underset{x \in X \subseteq \mathbb{R}^k}{\text{minimize}} \quad P(x) = \sum_{j=1}^n \frac{1}{T} \int_0^T (|\tau_j \dot{q}_j| + K \tau_j^2) dt, \quad (3)$$

$$\underset{x \in X \subseteq \mathbb{R}^k}{\text{minimize}} \quad 1/X_{DBM}, \quad (4)$$

subject to

$$g_1(x) \equiv q^j - q_{min}^j \geq 0, \quad (5)$$

$$g_2(x) \equiv q_{max}^j - q^j \geq 0, \quad (6)$$

$$g_3(x) \equiv 0.4 Nm - \text{mean}(\Delta \tau_{ij}^{max}) \geq 0, \quad (7)$$

$$g_4(x) \equiv \min(X_{DBM}^i) - 0.001 m \geq 0, \quad (8)$$

$$g_5(x) \equiv \min(Y_{DBM}^i) - 0.001 m \geq 0, \quad (9)$$

$$g_6(x) \equiv q_{LShoulderPitch}^{final} - q_{LShoulderPitch}^{initial} \geq 0, \quad (10)$$

$$g_7(x) \equiv q_{LElbowRoll}^{final} - q_{LElbowRoll}^{initial} \geq 0, \quad (11)$$

$$g_8(x) \equiv \min Y_{DBM}^{Avg} m - Y_{DBM}^{Avg} \geq 0, \quad (12)$$

$$x_i^L \leq x_i \leq x_i^U, \quad \text{with}$$

$$x_i^L = [0.25, -0.05, -0.05, 0.001, 0.001, -0.2, -0.2, 0.015, 0.4, 0, 1, 0.04, 0.2]^T,$$

$$x_i^U = [0.31, 0.05, 0.05, 0.2, 0.2, 0.2, 0.2, 0.030, 4, \pi/2, 2, 0.5, 1.5]^T,$$

$$q_{min}^j = -[1.14, 0.38, 1.53, 0.09, 1.19, 0.39, 0.79, 1.53, 0.10, 1.18, 0.76]^T,$$

$$\text{and, } q_{max}^j = [0.74, 0.79, 0.48, 2.11, 0.92, 0.76, 0.38, 0.48, 2.12, 0.93, 0.39]^T.$$

The number of decision parameters is denoted by k , which is 13 for SSP and 12 for DSP. x_1 represents hip height. x_2 and x_3 denote the initial and final

velocities associated with the hip height, respectively. x_4 and x_5 represent the initial and final sagittal velocities, whereas x_6 and x_7 indicate the initial and final lateral velocities. x_8 and x_9 denote the maximum swing height and time spent in SSP, respectively. x_{10} and x_{11} denote the left arm's initial and final shoulder pitch angles. x_{12} and x_{13} denote the left arm's initial and final elbow roll angles. The right arm will move opposite to the left arm. The j^{th} joint's movement is restricted within q_{min}^j rad and q_{max}^j rad. The joint angle values are starts from HipYawPitch, and other joints' values follow the order from the hip to ankle joint [29]. The walking cycle time is considered in ten equal parts. Superscripts min, Avg and i (in $min(X_{DBM}^i)$ and Y_{DBM}^{Avg}) denote the min DBM, mean DBM in i^{th} interval during gait cycle. $\Delta\tau_{ij}^{max}$ is the threshold value for torque fluctuation. j and i together denote j^{th} joint in i^{th} time interval. $^{min}Y_{DBM}^{Avg}$ during SSP is considered as 0.02 m.

The selection of gait parameters for optimization is a crucial step that requires careful consideration. Our approach involves careful consideration of various gait parameters, such as hip trajectory, swing leg trajectory, arm motion, and transition velocities, with the intention of addressing gaps identified in previous research. Based on the previous study conducted in this area by Gupta et al. [14], the first 9 gait parameters for SSP and 8 gait parameters for DSP have been retained. Four new specifically designed gait parameters have been introduced to control arm movement. Through the deliberate selection of these parameters, it is to be noted that the key regions have emerged through the deliberate selection of these parameters in both the SSP as well as DSP.

The objectives and nature of the DSP problem closely resemble those of the SSP problem, with a few notable differences. These include variations in the values of certain constraints, such as the minimum average DBM in the y direction ($^{min}Y_{DBM}^{Avg}$) taken as 0.05 m, as well as a change in the number of decision parameters. Specifically, in the DSP problem, the number of decision parameters is reduced to 12 from the 13 parameters present in the SSP formulation. The reduction in the number of decision parameters in the DSP problem is primarily attributed to the absence of the swing height parameter. In the DSP phase, the body weight is supported by both legs, namely the left leg ($[0.06, 0.05, 0]^T$) and the right leg ($[0.12, -0.05, 0]^T$), working simultaneously to move the torso from left to right leg while providing stability and support to the robot. The X_{DBM} represents the minimum DBM as explained in Fig. 3(f). The lower and upper limits for the last five decision variables are considered as from $[0.2, 0, 1, -0.50, -1.50]^T$ to $[2, \pi/2, 2, -0.04, -0.2]^T$. The rest of the decision parameters ($x_1 - x_7$) are similar to SSP with the exception of the maximum swing height.

There are eight constraints considered for the optimization process during both phases. The joints constraints ($g_1(x)$ and $g_2(x)$) restrict joint movements within their allowable ranges. The minimum change in torque constraints ($g_3(x)$) keeps the fluctuations within a predefined limit. $mean(\Delta\tau_{ij}^{max})$ denotes the mean of fluctuation of torque for j^{th} joint in i^{th} interval. Minimum DBM constraints ($g_4(x)$ and $g_5(x)$) keep the motion dynamically stable in x - and y -direction. A

minimum DBM of $0.001 m$ should always be maintained in both directions. Hand movement constraints ($g_6(x)$ and $g_7(x)$) would help in moving the arms according to the leg movement and in the right order. The average DBM in the y direction ($g_8(x)$) helps maintain a stability margin of $0.02 m$ during SSP and $0.05 m$ during DSP.

6 Results and Discussion

NSGA-II has been used to solve the SSP and DSP problem of the NAO humanoid robot for two objectives, viz. Average Power Consumption and Dynamic Balance Margin. The following NSGA-II parameters are found to get the better result. The distribution indices for crossover (η_c) and mutation (η_m) are taken as 20 and 50, respectively. Crossover probability and real-parameter mutation probability are set as 0.9 and 0.1, respectively. A population size of 152 and 200 generations are considered to get an optimal solution. Figs. 4 (a) and 4 (d) show PF for the SSP and DSP problems without using any knee-finding techniques. Figs. 4(b) shows the single-angle measure solutions obtained using knee-finding NSGA-IIs. Fig. 4(c) shows the knee solution obtained using a utility-based measure. The angle-based function can be easily implemented for $2-D$ cases, but the utility-based function gives the better results due to the number of well-distributed weight vectors. The four-angle measure can also be computed using a maximum of four-points slope method; to get a better focus on the knee region than single angle measure. The PF obtained during SSP has one knee region, which is useful to the DM. It suggests that the hip's initial and final position is crucial and can change the PF shape. The step length determines the hip movement during the SSP. Different close trajectories are available; most importantly, they are always dynamically stable. These trajectories fulfill the constraints of providing a single knee region during SSP.

Similarly, Figs. 4(e) and (f) show the obtained PF during DSP using the single-angle and utility approaches. In contrast to SSP, DSP produces a PF with two knee-like regions indicating two favored locations, since the support polygon (due to both legs being on the ground) has a larger area than in the SSP case. Two types of trajectories satisfy all of the stability constraints. One trajectory improves stability by requiring more power (an example of dynamic stability). The alternate trajectory uses less power since the robot is already stable (an example of static stability, as it moves very slowly while still satisfying the stability constraints) because both the legs are on the ground, which accounts for the presence of an additional knee-like region. Both the utility-based and angle-based methods are able to identify both knee regions. However, in both cases, the utility-based method is found to be better than the angle-based method in detecting multiple knee regions with well-distributed solutions.

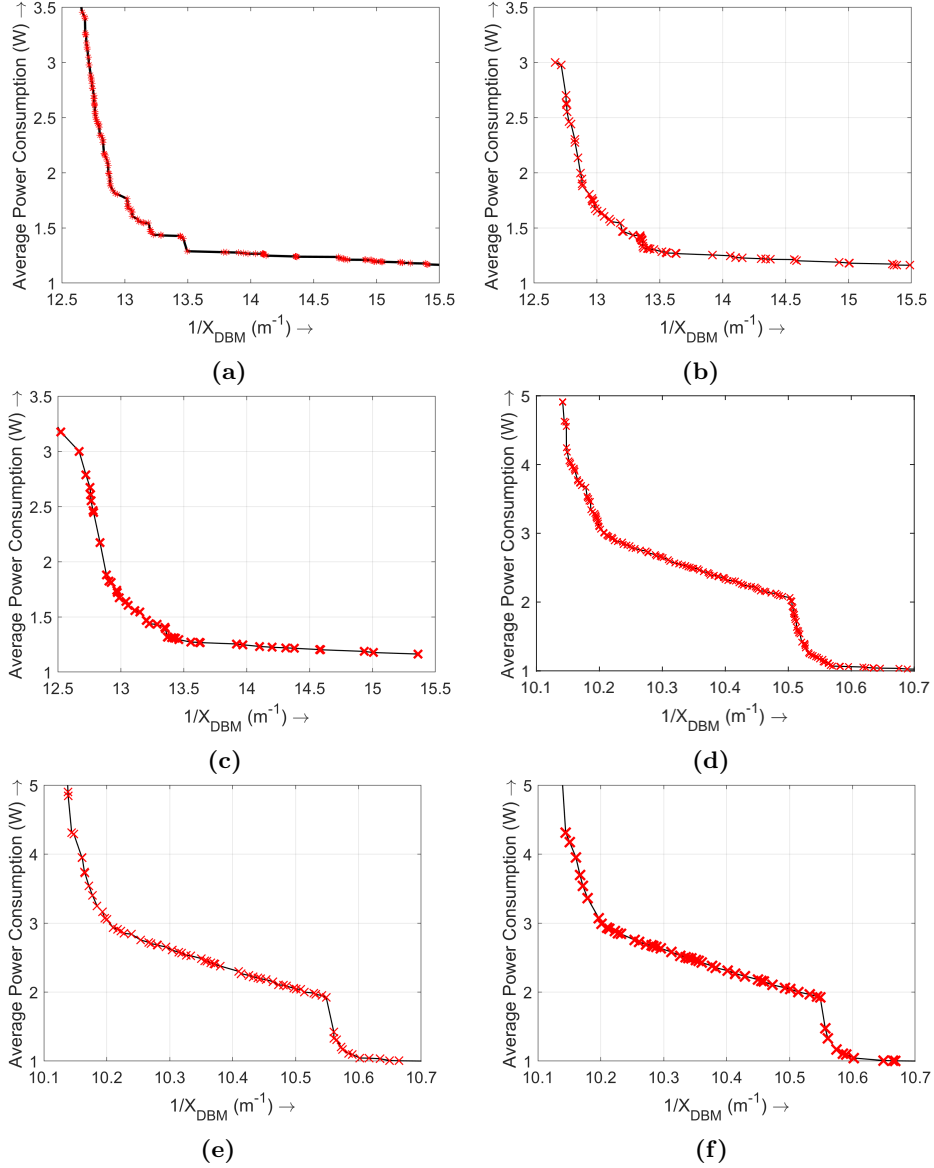


Fig. 4: SSP Problem: **a** NSGA-II SSP result. **b** single-angle measure. **c** utility-based measure on the gait cycle. DSP Problem: **d** NSGA-II DSP result. **e** single-angle measure. **f** utility-based measure on the gait cycle.

7 Conclusions

The modified NSGA-II knee-based technique has proven effective in reducing the search space and decreasing the decision maker’s workload during the SSP and DSP of the NAO humanoid robot’s gait cycle. If there is a bulge in the PF, this technique concentrates on the knee region, as verified on the test problem. While real-world problems may not contain an obvious knee bulge, they often have high trade-off areas where improvement in one objective results in significant deterioration of another. The SSP solutions concentrated around the knee region, with fewer solutions at the extremes. The DSP revealed two knee regions where solutions clustered. This demonstrates the ability of the knee-finding NSGA-II algorithm to locate key trade-off regions even for complex real-world optimization tasks.

It is worthwhile to note that the four-angle measure focused more heavily on the knee area compared to the single-angle approach. However, angle-based techniques rely on local neighborhood information, limiting their adaptability. In contrast, the utility-based method considers objective trade-offs more holistically, enabling better identification and focusing on knee regions. With sufficient weight vectors representing objective importance, the utility-based approach outperformed the angle-based method. Expanding the utility-based NSGA-II to many objective problems with additional criteria like power, stability, and torque fluctuations could reveal further trade-offs.

Overall, this research highlights effective mechanisms to locate key trade-off regions to aid decision-making in complex multi-objective optimization. The knee-finding NSGA-II techniques developed here facilitate practical implementation by reducing the solution space and guiding the decision-maker. Further work could expand these methods to improve performance across a wider range of real-world problems.

References

1. Afsar, B., Miettinen, K., Ruiz, A.B.: An artificial decision maker for comparing reference point based interactive evolutionary multiobjective optimization methods. In: International Conference on Evolutionary Multi-Criterion Optimization, pp. 619–631. Springer (2021)
2. Benítez-Hidalgo, A., Nebro, A.J., García-Nieto, J., Oregi, I., Del Ser, J.: jmetalpy: A python framework for multi-objective optimization with metaheuristics. *Swarm and Evolutionary Computation* **51**, 100,598 (2019)
3. Blank, J., Deb, K.: Pymoo: Multi-objective optimization in python. *IEEE Access* **8**, 89,497–89,509 (2020)
4. Branke, J., Deb, K., Dierolf, H., Osswald, M.: Finding knees in multi-objective optimization. In: International conference on parallel problem solving from nature, pp. 722–731. Springer (2004)
5. Das, I.: On characterizing the “knee” of the pareto curve based on normal-boundary intersection. *Structural optimization* **18**(2), 107–115 (1999)

6. Dau, V.H., Chew, C.M., Poo, A.N.: Achieving energy-efficient bipedal walking trajectory through GA-based optimization of key parameters. *International Journal of Humanoid Robotics* **6**, 609–629 (2009)
7. Deb, K., Gupta, S.: Understanding knee points in bicriteria problems and their implications as preferred solution principles. *Engineering optimization* **43**(11), 1175–1204 (2011)
8. Deb, K., Pratap, A., Agarwal, S., Meyarivan, T.: A fast and elitist multiobjective genetic algorithm: NSGA-II. *IEEE transactions on evolutionary computation* **6**(2), 182–197 (2002)
9. Deb, K., Tiwari, S.: Multi-objective optimization of a leg mechanism using genetic algorithms. *Engineering Optimization* **37**(4), 325–350 (2005). DOI 10.1080/03052150500066695. URL <https://doi.org/10.1080/03052150500066695>
10. Denavit, J., Hartenberg, R.S.: A kinematic notation for lower-pair mechanisms based on matrices (1955)
11. Durillo, J.J., Nebro, A.J.: jmetal: A java framework for multi-objective optimization, advances in engineering software. *IEEE Trans. Evol. Comput* **10**, 760–771 (2011)
12. Fu, K.S., Gonzalez, R.C., Lee, C.S.: *Robotics: Control, Sensing, Vision and Intelligence*. Tata McGraw-Hill Education (1987)
13. Gong, D., Yan, J., Zuo, G.: A review of gait optimization based on evolutionary computation. *Applied Computational Intelligence and Soft Computing* **2010** (2010)
14. Gupta, P., Pratihari, D.K., Deb, K.: Analysis and optimization of gait cycle of 25-dof NAO robot using particle swarm optimization and genetic algorithms. *International Journal of Humanoid Robotics* (2023, doi: 10.1142/S0219843623500111). URL <https://doi.org/10.1142/S0219843623500111>
15. Hadka, D.: *Platypus-multiobjective optimization in python* (2015)
16. Jesús Mejía: *Metaheuristics: High-performance metaheuristics for optimization coded purely in julia* (2022). URL <https://github.com/jmejia8/Metaheuristics.jl>. [Online; accessed 15-August-2022]
17. Kajita, S., Hirukawa, H., Harada, K., Yokoi, K.: *Introduction to Humanoid Robotics*, vol. 101. Springer (2014)
18. Li-Yang Wang, Liu, Z., Xiao-Jie Zeng, Zhang, Y.: Gait control of humanoid robots via fuzzy logic and iterative optimization. In: *Proceedings of the 30th Chinese Control Conference*, pp. 3931–3936. IEEE (2011)
19. Luo, X., Xia, D., Zhu, C.: Impact dynamics-based torso control for dynamic walking biped robots. *International Journal of Humanoid Robotics* **15**(03), 1850,004 (2018)
20. Mahmoodabadi, M.J., Taherkhorsandi, M.: Intelligent control of biped robots: optimal fuzzy tracking control via multi-objective particle swarm optimization and genetic algorithms. *AUT Journal of Mechanical Engineering* **4**(2), 183–192 (2020)
21. Muni, M.K., Parhi, D.R., Kumar, P.B., Sahu, C., Kumar, S.: Towards motion planning of humanoids using a fuzzy embedded neural network approach. *Applied Soft Computing* **119**, 108,588 (2022). DOI <https://doi.org/10.1016/j.asoc.2022.108588>. URL <https://www.sciencedirect.com/science/article/pii/S1568494622000990>
22. Pratihari, D.K.: *Fundamentals of Robotics*. Narosa Publishing House Pvt. Ltd. (2017)
23. PyGMO, I.D.: *Pykep: open source tools for massively parallel optimization in astrodynamics (the case of interplanetary trajectory optimization)*. In: *Proceedings of the Fifth International Conference on Astrodynamics Tools and Techniques, ICATT* (2012)

24. Rachmawati, L., Srinivasan, D.: Multiobjective evolutionary algorithm with controllable focus on the knees of the pareto front. *IEEE Transactions on Evolutionary Computation* **13**(4), 810–824 (2009)
25. Raj, M., Semwal, V.B., Nandi, G.C.: Multiobjective optimized bipedal locomotion. *International Journal of Machine Learning and Cybernetics* **10**, 1997–2013 (2019)
26. Rajendra, R., Pratihari, D.K.: Analysis of double support phase of biped robot and multi-objective optimization using genetic algorithm and particle swarm optimization algorithm. *Śadhanā* **40**, 549–575 (2015)
27. Seo, Y.J., Yoon, Y.S.: Design of a robust dynamic gait of the biped using the concept of dynamic stability margin. *Robotica* **13**(5), 461–468 (1995). DOI 10.1017/S0263574700018294
28. Silva, F.M., Machado, J.A.T.: Energy analysis during biped walking. pp. 59–64 (1999)
29. SoftBank Robotics Developer Center: Kinematics data: Links, joints, and body frames (2021). URL <https://developer.softbankrobotics.com/nao6/nao-documentation/nao-developer-guide/kinematics-data>. [Online; accessed 15-August-2021]
30. SoftBank Robotics Developer Center: The masses and COM positions for NAO (2021). URL <https://developer.softbankrobotics.com/nao-naoqi-2-1/nao-documentation/nao-technical-guide/nao-h25/h25-masses>. [Online; accessed 15-August-2021]
31. Tushar, Vundavilli, P.R., Pratihari, D.K.: Dynamically balanced ascending gait generation of a biped robot negotiating staircase. In: 2008 IEEE Region 10 and the Third international Conference on Industrial and Information Systems, pp. 1–6 (2008). DOI 10.1109/ICIINFS.2008.4798359
32. Uno, Y., Kawato, M., Suzuki, R.: Formation and control of optimal trajectory in human multijoint arm movement. *Biological Cybernetics* 1989 61:2 **61**, 89–101 (1989). DOI 10.1007/BF00204593. URL <https://link.springer.com/article/10.1007/BF00204593>
33. Van Veldhuizen, D.A., Lamont, G.B.: Multiobjective evolutionary algorithms: Analyzing the state-of-the-art. *Evolutionary computation* **8**(2), 125–147 (2000)
34. Vukobratović, M., Borovac, B.: Zero-moment point—thirty five years of its life. *International journal of humanoid robotics* **1**, 157–173 (2004)
35. Vundavilli, P.R., Sahu, S.K., Pratihari, D.K.: Dynamically balanced ascending and descending gaits of a two-legged robot. *International Journal of Humanoid Robotics* **4**, 717–751 (2007)
36. Vundavilli, P.R., Sahu, S.K., Pratihari, D.K.: Online dynamically balanced ascending and descending gait generations of a biped robot using soft computing. *International Journal of Humanoid Robotics* **4**, 777–814 (2007)
37. Yu, G., Jin, Y., Olhofer, M.: Benchmark problems and performance indicators for search of knee points in multiobjective optimization. *IEEE transactions on cybernetics* **50**(8), 3531–3544 (2019)
38. Zhang, K., Shen, C., He, J., Yen, G.G.: Knee based multimodal multi-objective evolutionary algorithm for decision making. *Information Sciences* **544**, 39–55 (2021)
39. Zhang, K., Yen, G.G., He, Z.: Evolutionary algorithm for knee-based multiple criteria decision making. *IEEE Transactions on Cybernetics* **51**(2), 722–735 (2019)